AJNR

Field, Coil, and Echo-Time Influence on Sensitivity and Reproducibility of Brain Proton MR Spectroscopy

M. Inglese, M. Spindler, J.S. Babb, P. Sunenshine, M. Law and O. Gonen

AJNR Am J Neuroradiol 2006, 27 (3) 684-688
http://www.ajnr.org/content/27/3/684

ORIGINAL RESEARCH

Field, Coil, and Echo-Time Influence on Sensitivity and Reproducibility of Brain Proton MR Spectroscopy

M. Inglese
M. Spindler
J.S. Babb
P. Sunenshine
M. Law
O. Gonen

BACKGROUND AND PURPOSE: Clinical MR imaging scanners now offer many choices of hardware configurations that were not available in the first 25 years of their existence. Our goal was to assess the influence of coil technology, magnetic field strength, and echo time (TE) on the sensitivity, reflected by the signal intensity-to-noise-ratio (SNR) and reproducibility of proton MR spectroscopy (^{1}H-MR spectroscopy).

MATERIAL AND METHODS: The SNR, the intersubject reproducibility, and the intrasubject reproducibility of *N*-acetylaspartate (NAA), creatine (Cr), and choline (Cho) levels were compared at the common TEs of 30, 144, and 288 ms, by using ^{1}H-MR spectroscopy in 6 volunteers at (1) 3T with a single-element quadrature (SEQ); (2) 1.5T with SEQ; and (3) 1.5T with a 12-channel phased-array (PA) head coil.

RESULTS: In terms of sensitivity, the best SNR for all metabolites was obtained at the shortest TE (30 ms). It was comparable between the 3 and 1.5T with the PA, but ~35% better than the 1.5T with SEQ. This SNR difference declined <25% at TE of 144 ms and to equity among all imagers at TE of 288 ms. Reproducibility, reflected in the coefficient of variation (CV), was best for NAA at TE of 288 ms, 15%–50% better than at TE of 30 ms in either gray (GM) or white matter (WM). The CV for Cr was best, at TE of 288 ms for GM, but its WM results were independent of TE. Metabolite level reproducibility did not depend on coil technology or magnetic field strength.

CONCLUSIONS: For the same coil type, the SNR of all major metabolites was ~35% better at 3T than at 1.5T. This advantage, however, was offset at 1.5T with a PA coil, making it a cost-effective upgrade for existing scanners. Surprisingly and counterintuitively, despite the lowest SNR, the best reproducibility was obtained at the longest TE (288 ms), regardless of field or coil.

In the first 2 decades of clinical neuro-MR imaging, the instrumentation offered by the mainstream manufacturer was limited to a magnetic field strength, B_0, of 1.5T and a single-element quadrature (SEQ) coil to its many variants. Although higher B_0, 3- to 4T scanners,[1–3] and custom multichannel phased arrays (PA) have been operational since the early 1990s,[4,5] neither technology was packaged into FDA-approved clinical products until nearly a decade later.

Each of these technologies can by itself increase the sensitivity, as reflected by the signal intensity-to-noise-ratio (SNR) per unit time of brain MR imaging and proton MR spectroscopic imaging (^{1}H-MR spectroscopy), via a different mechanism. Higher B_0 values can theoretically achieve linear improvements in field strength,[6,7] though T2 losses during the echo time (TE) reduce the actual gain to 20%–30% for doubling B_0 values from 1.5 to 3T.[8–11] The PA extends to the entire head the up to 10-fold SNR benefits from the improved filling-factor of surface coils.[12–14] Because these mechanisms are independent, their SNR advantages can be combined potentially for even greater overall gain.[15]

Although many ^{1}H-MR spectroscopy studies have examined the influence of B_0 or coil technology on the SNR,[16] few investigated the clinically more relevant quantity, reproducibility.[17–20] Even then, the focus was always on the performance of a specific hardware and sequence combination and not, to our knowledge, on optimizing both for reproducibility. In light of the clinical relevance of resolving "normal" from "pathological," the new choices of B_0 values, coils, sequence-parameters, and their substantial cost difference, establishing optimal setup for reproducibility for each configuration seems to be timely. Consequently, our aim was to evaluate the dependence of the reproducibility and the SNR of the major ^{1}H-MR spectroscopy observable metabolites: *N*-acetylaspartate (NAA), choline (Cho), and creatine (Cr) on the magnetic field strength, coil technology, and TE.

Received March 30, 2005; accepted after revision August 1.

From the Department of Radiology, New York University School of Medicine, New York, NY.

This work was supported by National Institutes of Health grants EB01015, NS050520, NS051623, and NS39135 and by the Martin S. Davis Research Fellowship Endowment from the National Multiple Sclerosis Society.

Address correspondence and reprint requests to Oded Gonen, PhD, Department of Radiology, New York University School of Medicine, 650 1st Ave, New York, NY 10016.

Methods

Subjects

We chose for this study a cohort of healthy young volunteers to minimize the "biologic noise." Specifically, we assumed that the physiologic variations of the concentrations of the different metabolites in analogous regions in their brains would be the smallest. Consequently, 6 healthy volunteers (3 women and 3 men; mean age, 26 years; age range, 22–28 years) were enrolled. The study was approved by our institutional review board, and each subject was briefed on the procedure they were about to undergo and gave written informed consent.

MR Imaging and ^{1}H-MR Spectroscopy Acquisition

The experiments were conducted on 3 different MR scanners: (1) A 3T head-only imager with a SEQ transmit-receive head coil; (2) a 1.5T whole-body instrument with a SEQ receive-only coil; and (3) a 1.5T

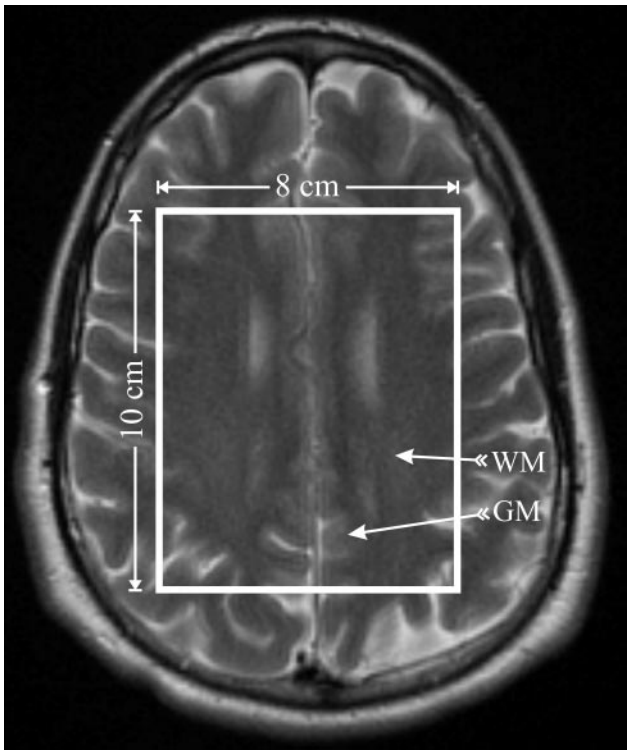

Fig 1. Axial, T2-weighted MR imaging of a healthy female volunteer, superimposed with the $8_{LR} \times 10_{AP} \times 1.5_{IS}$ = 120 mL MR spectroscopy VOI (*solid white outline*), which was placed over similar anatomy (superior margin of the lateral ventricles) in all 6 subjects by a neuroradiologist. The VOI was partitioned into $8_{LR} \times 10_{AP}$ voxels, 1.5 mL each. *Arrows* indicate the WM and GM voxels selected for the analyses in each subject.

whole-body with a 12-channel receive-only PA head coil. All scanners were from the same manufacturer and used in their standard commercial brain MR imaging/MR spectroscopy configuration.

Fifteen 5-mm-thick axial T2-weighted (retention time [TR]/TE = 6000/99 ms; 90° flip angle; 256 × 256 matrix; 24 × 24 cm^2 field of view [FOV]) images were used to guide an 8-cm left-right × 10-cm anteroposterior × 1.5-cm inferior-superior volume of interest (VOI). It was placed onto a similar brain location, shown in Fig 1, in every subject by an experienced neuroradiologist (M.L.). The VOI was excited by using point-resolved spectroscopy (PRESS) and partitioned into the superior border of the lateral ventricles $8_{LR} \times 10_{AP}$ voxels, 1 × 1 × 1.5 mL each, with 16 × 16 2D chemical shift imaging (CSI) along a $16_{LR} \times 16_{AP}$-cm FOV, with the same radio-frequency pulses, section-select, crusher gradients strengths, slew-rates, and duration on all 3 imagers. The signal intensity was acquired at 500-Hz bandwidth with 1024 complex points at 1.5T and 1 kHz with 2048 points at 3T, to yield equal (1 Hz per point) spectral resolution at each B_0.

The 2D ^{1}H-MR spectroscopy in the VOI was repeated at short, intermediate, and long TEs (30, 144, and 288 ms), back to back, all with the same TR (1850 ms) for each of the 6 subjects. Every subject was scanned on all 3 instruments in the same day.

^{1}H-MR Spectroscopy Quantification

Residual water was removed from the MR spectroscopy data in the time domain,[21] and the signals were apodized with a 2-Hz lorentzian, voxel-shifted to align the CSI grid with the VOI of the NAA,[22] and Fourier-transformed in the spatial and spectral directions. Automatic frequency, zero, and first-order phase corrections were made by using the NAA and Cr peaks for reference in each voxel.[10] Relative amounts of the *i*th (= NAA, Cr, or Cho) metabolite in the *j*th (= 1 . . . 80) voxel of the *k*th (= 1 . . . 6) subject, Q_{ijk}, were estimated from the spectral peak areas, S_{ijk}, by using parametric spectral modeling and least-squares optimization.[23] The Q_{ijk}'s were converted into absolute amounts by repeating the ^{1}H-MR spectroscopy on a reference 3-L sphere of 0.033 mol of NAA in water as[24,25]

$$1) \qquad Q_{ijk} \approx \frac{S_{ijk}}{\bar{S}_R} \cdot 0.033 \quad \text{Moles},$$

where $\bar{S}_R$ is the reference's voxels average NAA peak area. Because 2 coils were receive-only, no corrections for loading were made. Because the same subjects were compared in all imagers, we assume that the errors associated with this omission had little effect on the conclusions.

The Q_{ijk} from Equation (1) were corrected for the differences in the relaxation times between the reference phantom T1/T2 values (NAA only, $T1^{ref}$ = 1.4 seconds, $T2^{ref}$ = 0.5 seconds at 1.5T) and those reported in vivo: NAA T1/T2 = 1.4/0.43 seconds; Cr = 1.6/0.21 seconds; Cho = 1.2/0.36 seconds at 1.5T[26,27] and similar T1 but shorter T2s of 230, 150, and 186 ms, respectively,[28,29] at 3T, by using[25]

$$2) \quad Q_{ijk}^{corrected} \approx Q_{ijk} \cdot \left(1 - \frac{TE \cdot (T_2^i - T_2^{ref})}{T_2^i \cdot T_2^{ref}}\right) \cdot \frac{T_1^{ref}}{T_1^i}$$

i = NAA, Cho or Cr.

Because similar brain locations were compared in all subjects, as shown in Fig 1, possible regional T1 or T2 variations[29] were ignored. SNR, defined as the ratio of the peak height, h_{ijk} (= $S_{ijk}/T2^i$)[30] to the root mean square of the noise,[31] was automatically estimated in each voxel.

Statistical Analyses

Mixed model analysis of variance was used to compare imagers and TEs with respect to the mean, SNR, and coefficient of variations (CV = SD/average) of the NAA, Cr, and Cho levels. A separate analysis was conducted for each outcome (mean, SNR, CV) of each metabolite within each tissue type (gray matter [GM] or white matter [WM]). In each case, the dependent variable comprised the outcome levels observed for all subjects and the model included machine and TE as fixed classification factors as well as the term representing their interaction. The covariance structure was modeled by assuming observations to be correlated or independent when acquired from the same or different subjects, respectively, with the strength of correlation dependent on whether the data were from the same session and by allowing the error variance to differ across machines and TEs. Within this framework, likelihood ratio tests were used to compare machines and TEs with respect to CV, whereas Tukey honestly significant difference (HSD) procedure was used to make all pairwise comparisons among machines and TEs in terms of mean levels and SNR while maintaining the family-wise significance level for the set of comparisons at or below the 5% level.

Results

Overall, for 6 (subjects) × 3 (TEs) × 3 (scanners) this study yielded 54 ^{1}H-MR spectroscopy datasets. The SNRs for the NAA, Cr, and Cho, in the GM and WM, 3 imagers, 2 coil types, and 3 TEs, are compiled in Table 1 and the CVs in Table 2. Because of numerous possible pairwise statistical comparisons among these variables, we summarize, for the sake of simplicity, only the specific findings pertaining to sensitivity and reproducibility.

Table 1: Signal intensity-to-noise-ratio (SNR) values in gray matter (GM) and white matter (WM) from the volunteers for selected metabolites

Metabolite	Tissue	Imager	SNR at TE (ms) 30	144	288
N-acetylaspartate	GM	3 T	191.6 ± 21.4	118.6 ± 14.5	88.5 ± 12.6
	GM	1.5 T + PA	227.4 ± 23.1	142.2 ± 14.9	96.7 ± 14.6
	GM	1.5 T	131.2 ± 18.1	106.2 ± 19.5	73.0 ± 20.6
	WM	3 T	283.4 ± 38.5	168.4 ± 15.9	90.1 ± 10.8
	WM	1.5 T + PA	245.7 ± 24.0	143.9 ± 16.0	108.8 ± 12.1
	WM	1.5 T	149.9 ± 19.0	102.9 ± 9.6	78.9 ± 12.1
Creatine	GM	3 T	110.4 ± 20.2	58.6 ± 9.9	33.6 ± 8.2
	GM	1.5 T + PA	125.8 ± 9.2	67.4 ± 11.1	28.1 ± 9.3
	GM	1.5 T	70.4 ± 11.4	43.2 ± 11.5	22.9 ± 11.6
	WM	3 T	91.0 ± 12.9	66.1 ± 8.5	22.9 ± 5.9
	WM	1.5 T + PA	103.3 ± 9.4	46.8 ± 6.3	24.8 ± 5.7
	WM	1.5 T	61.5 ± 5.0	36.9 ± 2.1	17.9 ± 5.3
Choline	GM	3 T	17.2 ± 2.8	16.1 ± 2.5	11.2 ± 2.1
	GM	1.5 T + PA	16.9 ± 3.0	15.4 ± 3.2	10.2 ± 2.2
	GM	1.5 T	12.5 ± 2.7	12.1 ± 2.8	6.8 ± 3.1
	WM	3 T	38.1 ± 3.0	27.8 ± 4.6	11.1 ± 1.3
	WM	1.5 T + PA	36.8 ± 3.3	23.0 ± 1.3	15.0 ± 2.1
	WM	1.5 T	18.7 ± 2.2	15.0 ± 2.5	7.0 ± 2.2

NOTE:—TE indicates echo time (values are mean ± SD); PA, phased array.

Table 2: Within-subject CVs for selected metabolites at different echo times (TE) in gray matter (GM) and white matter (WM) of volunteers

Metabolite	Tissue	TE (ms)	CV (%) 3T + SEQ	1.5T + PA	1.5T + SEQ
N-acetylaspartate	GM	30	10.54	9.11	8.72
	GM	144	7.00	5.48	7.21
	GM	288	8.49	5.57	4.80
	WM	30	9.11	9.59	5.66
	WM	144	8.60	7.48	3.61
	WM	288	4.37	4.90	4.00
Creatine	GM	30	27.50	8.43	12.45
	GM	144	9.06	12.21	15.87
	GM	288	7.81	10.63	8.83
	WM	30	10.72	10.44	5.97
	WM	144	12.00	11.00	15.30
	WM	288	10.95	12.45	14.70
Choline	GM	30	9.22	12.61	13.04
	GM	144	23.28	23.24	12.69
	GM	288	10.82	23.32	13.49
	WM	30	8.72	11.23	11.79
	WM	144	22.69	13.96	17.75
	WM	288	8.31	11.70	13.64

Note:—SEQ indicates single-element quadrature; PA, phased array.

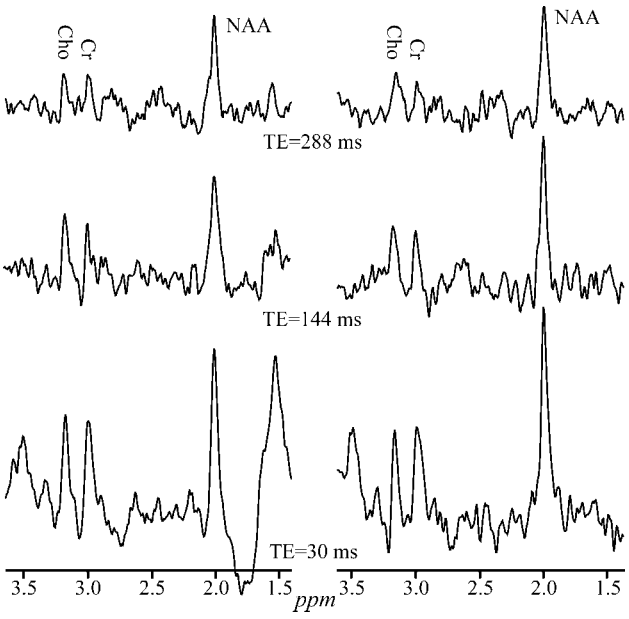

Fig 2. Real part of the GM ^{1}H-MR spectrum acquired at 1.5T with a SEQ coil at short (30 ms), intermediate (144 ms), and long TE (288 ms) in 2 female volunteers, displayed on common intensity (vertical) and indicated chemical shift (parts per million [ppm]) scales. Note the consistent pattern of increasing NAA, Cr, and Cho SNRs with decreasing TE in both subjects and the between-subjects spectra feature consistency.

Sensitivity (SNR)

It was no surprise that the best SNRs, compiled in Table 1, were obtained at the short TE (30 ms) for all metabolites, magnetic fields, tissue types, and coil technology, as demonstrated in Fig 2. It was quite a surprise, however, that the SNR at 3T + SEQ coil was statistically indistinguishable from that of a 1.5T imager with PA. Both were significantly better (~50%) than that of the 1.5T with SEQ coil, as shown in Fig 3. The similarity of the SNRs at 3T and 1.5T with PA recurred at the intermediate TE (144 ms) but they were now only <25% better than the 1.5T with SEQ. At the long TE (288 ms) the SNRs of all metabolites were on par regardless of field or coil.

Reproducibility (CV)

Within-subject reproducibility, expressed as CVs, is compiled in Table 2 as functions of B_0, tissue type, metabolite, and coil technology. To our astonishment, despite the lowest SNR, the best reproducibility was obtained at the longest TE (288 ms) for all metabolites, tissue type field, or coil technology. The reproducibility of NAA was 15%–50% worse (larger CVs) at the shortest TE (30 ms) across all imagers. This pattern of longer TE associated with better reproducibility was also observed for Cr in the GM, whereas its WM results were indistinguishable across all TEs and imagers. The reproducibility of the Cho concentrations was similar in both GM and WM at 3T, ~30% better than at 1.5T, regardless of coil technology.

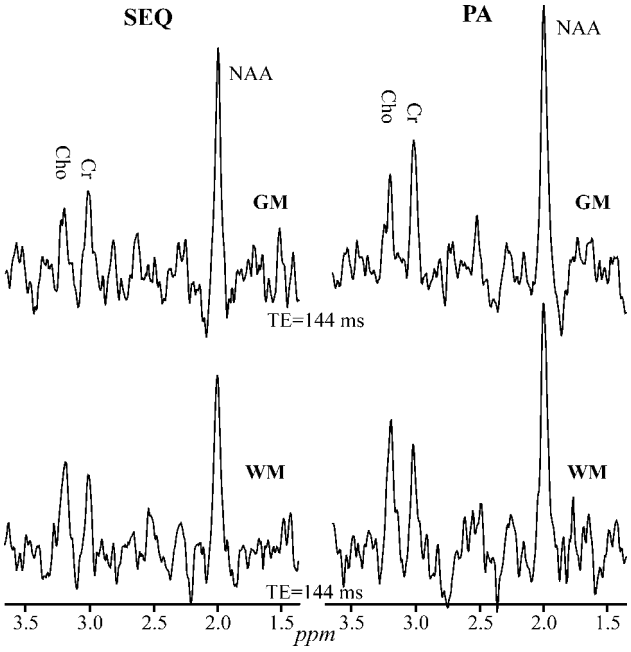

Fig 3. Comparison between the real part of the GM (top) and WM (bottom) ^{1}H-MR spectroscopy (TE = 144 ms) on common intensity and ppm scales, acquired from the same 2 voxels in a male volunteer at 1.5T with SEQ (*left*) and PA (*right*) coils. Note the higher SNRs for *all* metabolites in both GM and WM at with the PA versus SEQ coil.

Discussion

Our spectroscopic tool of choice for this comparison was 2D multivoxel ^{1}H-MR spectroscopy over the simpler more common single-voxel (SV) variants for 2 reasons: first, this technology facilitates much smaller voxels—typically <1 mL for the former versus >3 mL for the latter—which translate to much better spatial resolution. Second, we also wished to exploit the voxel-shift property of CSI,[22] to be able to position voxels, in postprocessing, as precisely as possible over the same anatomy across all subjects. We assume, on the basis of the literature, that variations would have been smaller if larger voxels had been used, because of smaller GM/WM/CSF partial volume impact on their content.[20] However, this would have come at the cost of lower spatial resolution, making "mostly GM" voxels, for example, more difficult to define.

Because the new clinical MR imaging scanners now offer a wide selection of hardware configurations and performance choices that were not available in the past, the aim of this study was to investigate the influence of coil technology, B_0, and TE on the sensitivity and reproducibility (SNR and CV) of ^{1}H-MR spectroscopy. The goal was to identify hardware and methodology configurations that led to better ^{1}H-MR spectroscopy in the brain (ie, what is the current "best" and the best way to achieve it).

Although a linear SNR increase with B_0 was theoretically predicted for ^{1}H-MR spectroscopy,[32,33] it was not actually realized. Lower-sensitivity coils, poorer shimming, and shorter T2s combine to reduce the expected gain to a more realistic 25%–50%, depending on the TE.[9,10,34] Therefore, our a priori expectation was that the higher (3T) field imager will also yield similar SNR improvements over the 1.5T imagers. Indeed, (1) for the *same* coil technology, the 3T yielded better SNR than its 1.5T counterpart, which is consistent with previous reports,[9,10] and (2) the best SNR for all metabolites and tissue types for a respective scanner was obtained at the shortest TE (30 ms), as shown in Table 1. That high field advantage, however, was offset by the PA coil on the 1.5T imager, which indicates that the latter is also worth 25%–50% SNR gain, but at a cost that is an order of magnitude lower. This was further corroborated by comparing the 2 1.5T scanners (ie, the SEQ vs PA coils) with the latter offering ~50% better SNR over the former (Table 1). Therefore, although a PA coil was not offered by the manufacturer for our 3T imager, its stands to reason that the best SNR overall would have been attained with it at the higher B_0.

Despite the SNR gain, the PA coil is not without its own disadvantages compared with transmit-receive SEQ coils. For MR spectroscopy applications, PA coils suffer in 3 main areas: first, their receive-only nature precludes straightforward, reciprocity-based loading corrections, detracting from the precision of intersubject absolute quantification; second, the consequent requirement for body-coil transmit restricts the strength of the radio-frequency fields attainable with it and greatly increases the power deposition (SAR); third, the different local receive sensitivity profiles of PA coils may lower the precision of their regional, intrasubject, absolute-level comparisons. Corrections for the first and third issues, especially for multivoxel arrays, is complex[35,36] and, in clinical settings, unlikely to be implemented by any manufacturer in the near future.

The most surprising finding in this study was that the best reproducibility was obtained at the longest TE (288 ms), where the SNR was worst, regardless of metabolite, tissue type, magnetic field, or coil technology. Our intuitive expectation was that with better SNR, obtained at the shorter TE, we could expect to better distinguish smaller changes. Because clinical applications require differentiating reliably and consistently "normal" from "abnormal," reproducibility is arguably more useful than SNR. Consequently, for current clinical applications—especially longitudinal or comparative studies focused on NAA, Cr, and Cho—the longer TEs are better performers, even though modern imagers with their fast shielded gradients and efficient transmit-receive coils could produce TEs more than an order of magnitude shorter.

In retrospect, several reasons could account for this counterintuitive finding. First, the more undulating baseline characteristics of shorter TEs—shown in Figs 2 and 4—could add random quantification noise. This hypothesis is supported by the fact that the greatest benefactor from this improvement is the NAA (Table 2), which is also the closest to the offending leaking-lipid resonances. Second, several brain macromolecular metabolites that give rise to the broad resonances[37] underlie primarily the NAA, and only to a lesser extent the Cr and Cho peaks. Compared with the metabolites of interest, these macromolecules undergo more rapid T2 decay into the noise at long TEs, increasing the precision of numeric fitting. Finally, the extraneous lipids signals which may "leak" into the VOI also experience T2 decay at long TEs, yielding a flatter baseline and, consequently, more reproducible quantification especially, again, for the NAA, as demonstrated in Figs 2 and 4.

Conclusion

Our data indicate that long TEs yield better reproducibility, which is arguably the most valuable attribute for clinical ap-

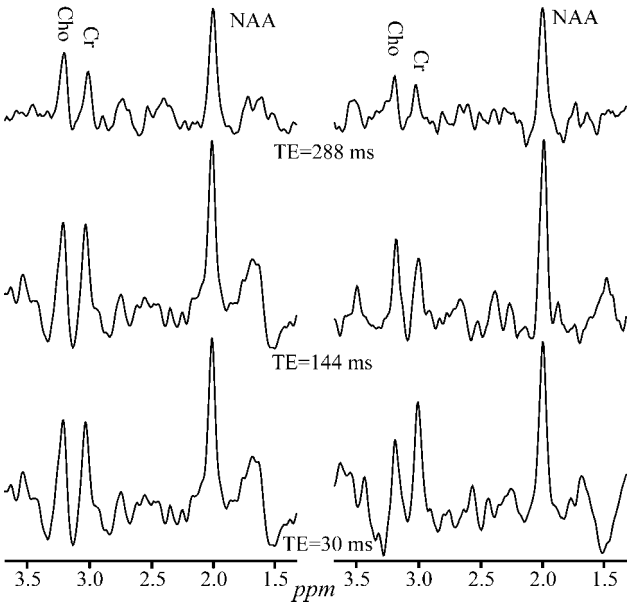

Fig 4. Real part of the GM ^{1}H-MR spectra, at 3T with SEQ coil, from 2 healthy male volunteers, at short, intermediate, and long TEs, displayed on common intensity and chemical shift scales. Note the reduced baseline undulations at the longest TE (288 ms) in both subjects compared with the intermediate and short TEs.

plications. Therefore, because setting long TEs (270 or 288 ms) is a trivial user setting at scan time, this could be the preferred choice for those clinical applications focusing on metabolites with long T2 singlet peaks. In addition, the SNR gain afforded by a PA coil upgrade is very cost-effective (~50%). Most important, on the basis of our findings, we assume the combination of a 3T and a PA coil, not available to us in this study, holds the most promise of dramatically enhancing performance from the B_0 doubling of these new high-field imagers with anticipated results potentially ushering in a new "gold standard."

References

1. Mason GF, Pan JW, Ponder SL, et al. **Detection of brain glutamate and glutamine in spectroscopic images at 4.1 T.** *Magn Reson Med* 1994;32:142–45
2. Ewing JR, Warner R, Helpern JA. **A cylindrically symmetric magnetic shield for a large-bore 3.0 Tesla magnet.** *Magn Reson Med* 1993;29:398–401
3. Ugurbil K, Garwood M, Ellermann J, et al. **Imaging at high magnetic fields: initial experiences at 4 T.** *Magn Reson Q* 1993;9:259–77
4. Roemer PB, Edelstein WA, Hayes CE, et al. **The NMR phased array.** *Magn Reson Med* 1990;16:192–225
5. Hayes CE, Hattes N, Roemer PB. **Volume imaging with MR phased arrays.** *Magn Reson Med* 1991;18:309–19
6. Ocali O, Atalar E. **Ultimate intrinsic signal-to-noise ratio in MRI.** *Magn Reson Med* 1998;39:462–73
7. Gruetter R, Weisdorf SA, Rajanayagan V, et al. **Resolution improvements in in vivo 1H NMR spectra with increased magnetic field strength.** *J Magn Reson* 1998;135:260–64
8. Bartha R, Drost DJ, Menon RS, et al. **Comparison of the quantification precision of human short echo time (1)H spectroscopy at 1.5 and 4.0 Tesla.** *Magn Reson Med* 2000;44:185–92
9. Barker PB, Hearshen DO, Boska MD. **Single-voxel proton MRS of the human brain at 1.5 T and 3.0 T.** *Magn Reson Med* 2001;45:765–69
10. Gonen O, Gruber S, Li BS, et al. **Multivoxel 3D proton spectroscopy in the brain at 1.5 versus 3.0 T: signal-to-noise ratio and resolution comparison.** *AJNR Am J Neuroradiol* 2001;22:1727–31
11. Li BS, Regal J, Gonen O. **SNR versus resolution in 3D 1H MRS of the human brain at high magnetic fields.** *Magn Reson Med* 2001;46:1049–53
12. Wright SM, Wald LL. **Theory and application of array coils in MR spectroscopy.** *NMR Biomed* 1997;10:394–410
13. Noworolski SM, Nelson SJ, Henry RG, et al. **High spatial resolution 1H-MRSI and segmented MRI of cortical gray matter and subcortical white matter in three regions of the human brain.** *Magn Reson Med* 1999;41:21–29
14. Wald LL, Moyher SE, Day MR, et al. **Proton spectoscopic imaging of the human brain using phased array detectors.** *Magn Reson Med* 1995;34:440–45
15. Hinton DP, Wald LL, Pitts J, et al. **Comparison of cardiac MRI on 1.5 and 3.0 Tesla clinical whole body systems.** *Invest Radiol* 2003;38:436–42
16. Di Costanzo A, Trojsi F, Tosetti M, et al. **High-field proton MRS of human brain.** *Eur J Radiol* 2003;48:146–53
17. Charles HC, Lazeyras F, Tupler LA, et al. **Reproducibility of high spatial resolution proton magnetic resonance spectroscopic imaging in the human brain.** *Magn Reson Med* 1996;35:606–10
18. Tedeschi G, Bertolino A, Campbell G, et al. **Reproducibility of proton MR spectroscopic imaging findings.** *AJNR Am J Neuroradiol* 1996;17:1871–79
19. Brooks WM, Friedman SD, Stidley CA. **Reproducibility of 1H-MRS in vivo** *Magn Reson Med* 1999;41:193–97
20. Li BS, Babb JS, Soher BJ, et al. **Reproducibility of 3D proton spectroscopy in the human brain.** *Magn Reson Med* 2002;47:439–46
21. Marion D, Ikura M, Bax A. **Improved solvent suppression in one- and two-dimensional NMR spectra by convolution of time domain data.** *J Magn Reson* 1989;84:425–30
22. Vigneron DB, Nelson SJ, Murphy-Boesch J, et al. **Chemical shift imaging of human brain: axial, sagittal, and coronal P-31 metabolite images.** *Radiology* 1990;177:643–49
23. Soher BJ, Young K, Govindaraju V, et al. **Automated spectral analysis. III. Application to in vivo proton MR spectroscopy and spectroscopic imaging.** *Magn Reson Med* 1998;40:822–31
24. Soher BJ, van Zijl PC, Duyn JH, et al. **Quantitative proton MR spectroscopic imaging of the human brain** *Magn Reson Med* 1996;35:356–63
25. Inglese M, Li BS, Rusinek H, et al. **Diffusely elevated cerebral choline and creatine in relapsing-remitting multiple sclerosis.** *Magn Reson Med* 2003;50:190–95
26. Barker PB, Blackband SJ, Chatham JC, et al. **Quantitation of proton NMR spectra of the human brain using tissue water as an internal concentration reference.** *NMR Biomed* 1993;6:89–94
27. Kreis R, Ernst T, Ross BD. **Absolute quantitation of water and metabolites in the human brain. II. Metabolite concentrations.** *J Magn Reson Ser B* 1993;102:9–19
28. Traber F, Block W, Lamerichs R, et al. **1H metabolite relaxation times at 3.0 Tesla: measurements of T1 and T2 values in normal brain and determination of regional differences in transverse relaxation.** *J Magn Reson Imaging* 2004;19:537–45
29. Ethofer T, Mader I, Seeger U, et al. **Comparison of longitudinal metabolite relaxation times in different regions of the human brain at 1.5 and 3 Tesla.** *Magn Reson Med* 2003;50:1296–301
30. Hoult DI. **The NMR receiver: a description and analysis of design.** *Prog NMR Spec* 1978;12:41–77
31. Ernst RR, Bodenhausen G, Wokaun A. *Principles of nuclear magnetic resonance in one and two dimensions.* Oxford: Clarendon Press; 1987:152
32. Hoult DI, Lauterbur PC. **The sensitivity of the zeugmatographic experiment involving human samples.** *J Magn Reson* 1979;34:425–33
33. Edelstein WA, Glover GH, Hardy CJ, et al. **The intrinsic signal-to-noise ratio in NMR imaging.** *Magn Reson Med* 1986;3:604–18
34. Kantarci K, Reynolds G, Petersen RC, et al. **Proton MR spectroscopy in mild cognitive impairment and Alzheimer disease: comparison of 1.5 and 3 T.** *AJNR Am J Neuroradiol* 2003;24:843–49
35. Murphy-Boesch J, Jiang H, Stoyanova R, et al. **Quantification of phosphorus metabolites from chemical shift imaging spectra with corrections for point spread effects and B1 inhomogeneity.** *Magn Reson Med* 1998;39:429–38
36. Jost G, Harting I, Heiland S. **Quantitative single-voxel spectroscopy: the reciprocity principle for receive-only head coils.** *J Magn Reson Imaging* 2005;21:66–71
37. Hwang JH, Graham GD, Behar KL, et al. **Short echo time proton magnetic resonance spectroscopic imaging of macromolecule and metabolite signal intensities in the human brain.** *Magn Reson Med* 1996;35:633–39